



# Research on Direct Speed Control Strategy for Maximum Power Point Tracking (MPPT) of Wind Turbines

Yaolin Lou<sup>a\*</sup>, Shubao Yang<sup>b</sup>, Mengxiao Wang<sup>a</sup>, Chenxi Wu<sup>c\*</sup>

- 5 <sup>a</sup>School of Electrical Engineering, Zhejiang University of Water Resources and Electric Power, Hangzhou 310018, China;  
<sup>b</sup>China Resources New Energy (Balikun) Co., Ltd., Hami City 839000, China;  
<sup>c</sup>Hangzhou Dianzi University, Hangzhou 310018, China

*Correspondence to:* Yaolin Lou(louyl@zuwe.edu.cn); Chenxi Wu (wuchenxi@hdu.edu.cn)

10 **Abstract.** Maximum Power Point Tracking (MPPT) below the rated wind speed is a key technology to improve the wind energy utilization efficiency of wind turbines. The existing commercial optimal torque control strategy is essentially an indirect speed control method, which has such problems as lacking optimal speed tracking error term, having non-adjustable convergence speed, and invalid control logic in the constant speed zone. To address the above shortcomings, this paper proposes a dynamic optimal speed estimation method based on the generator electromagnetic torque by analyzing the aerodynamic torque characteristics of the wind rotor under different wind speeds and the torque-speed operation trajectory of the generator at each maximum power tracking point, in accordance with the principle of the balance between aerodynamic torque and generator torque at the maximum power point. Taking this optimal speed as the control target, a direct speed controller based on speed deviation feedback is designed to achieve unified control of both constant speed zone and variable speed zone. A MATLAB/Simulink simulation model was built based on a 1.5 MW variable-speed variable-pitch wind turbine, and simulation verification was carried out under the conditions of gradient wind and turbulent wind in the minimum speed zone, variable speed zone and maximum speed zone, followed by field tests in wind farms. The results show that the proposed direct speed control strategy can stably realize MPPT under full operating conditions, effectively avoid torque and power oscillation, and keep the wind energy utilization coefficient stable at around 0.49. Moreover, it features simple control logic, can adapt to smooth switching of different wind speed conditions, and has good engineering application prospects.

25

**Keywords:** Wind Turbines; Maximum Power Point Tracking (MPPT); Direct Speed Control; Dynamic Optimal Speed; PI Controller; Wind Energy Utilization Coefficient

## 1 Introduction

30 Wind energy, characterized by significant stochasticity and volatility (Lin and Chen, 2019; Chen et al., 2022), exhibits continuously fluctuating wind speeds across temporal scales. The harvesting efficiency of wind energy depends not only on instantaneous wind speed magnitude but also on the control methodologies implemented in wind turbine systems. For large-



scale variable-speed wind turbines operating below rated wind speeds, the maximum power point tracking (MPPT) strategy (Chen et al., 2021; Lou et al., 2019; Zhou et al., 2023; Fathabadi, 2016; Abdullah et al., 2012) is typically employed to maintain turbine operation at optimal power points, thereby maximizing energy capture and enhancing utilization efficiency. Conversely, under supra-rated wind speed conditions, pitch control mechanisms are activated to stabilize power output (Tian et al., 2023).

Due to the stochastic nature of wind speed and nonlinear aerodynamic characteristics of rotor systems, achieving precise maximum power point tracking (MPPT) presents significant technical challenges. Consequently, the development of MPPT control strategies for wind turbines operating under-rated wind speed conditions remains one of the core technologies in wind turbine control systems (Ye, 2015; Fathabadi, 2017; Apata and Oyedokun, 2020). Current mainstream MPPT methodologies primarily include: Tip-Speed Ratio (TSR) control (Wang et al., 2019; Volosenescu, 2021; Zouheyr et al., 2021), Hill Climbing Search (HCS) algorithm (Zhang et al., 2012; Zhang et al., 2012), Optimal Torque Control (OTC) method (Chen et al., 2022; Zhang, 2019). The Tip-Speed Ratio (TSR) control method follows a straightforward design principle: by continuously measuring real-time wind speed, it dynamically computes the optimal rotational speed as the control target to achieve maximum power point tracking. However, practical limitations arise because anemometers are typically mounted on the nacelle, positioned 3–4 meters upstream of the rotor plane. This configuration introduces measurement inaccuracies due to rotor wake effects and temporal lag, rendering the acquired wind speed data unrepresentative of the effective wind speed at the rotor plane. Consequently, such measurements cannot be reliably utilized for turbine control. In contrast, the Hill Climbing Search (HCS) algorithm operates independently of wind speed measurements or turbine-specific parameters. By applying rotational speed perturbations and analyzing subsequent power gradients, it can adaptively track the MPPT. While demonstrating efficacy in small-scale wind turbines, this method proves inadequate for large-scale turbines with high rotational inertia, where transient response delays and mechanical stress constraints critically degrade its tracking stability.

The Optimal Torque Control (OTC) method is currently the most widely adopted MPPT strategy in commercial large-scale wind turbines. This control approach operates by continuously setting the generator torque (braking torque) proportional to the square of the generator rotational speed. Under an assumed constant wind speed condition, the generator torque is predetermined as the optimal aerodynamic torque. When the drive train reaches steady-state operation, the resultant generator speed converges to its optimal value. Essentially, this method implements an indirect speed control (ISC) mechanism without explicit speed regulation. The Optimal Torque Control (OTC) strategy eliminates the need for real-time wind speed measurements while maintaining smooth torque reference generation. However, this controller inherently lacks three critical components: Predefined optimal rotational speed setpoints; Speed error feedback terms; Adjustable parameters for tuning convergence rate; These structural deficiencies pose significant challenges in both controller stability analysis and performance enhancement.

Due to grid-synchronization speed constraints and rated speed limitations, wind turbines operating below rated wind speeds typically exhibit two distinct constant-speed operation zones and one variable-speed region. Within the variable-speed region, the Optimal Torque Control (OTC) strategy—where generator torque maintains a quadratic relationship with rotational speed—can be effectively implemented. However, this torque-speed proportionality ceases to hold in the constant-speed zones,



where the generator operates under fixed rotational speed thresholds. Consequently, the MPPT methodology based solely on OTC cannot be directly deployed in practical wind turbine controllers without additional adaptive compensation mechanisms.

To apply the optimal torque method in wind turbine controllers, Yang and Liu (2014) proposes a speed-torque look-up table strategy, where the generator torque value can be retrieved based on the current generator speed. However, the look-up table method reduces power generation near the constant speed region. Lou et al. (2018) realizes a method based on the proportional-integral (PI) controller output with dynamic torque limits by designing a switching logic between the minimum speed and rated speed, enabling the generator torque to vary along a quadratic curve trajectory and achieving a complete implementation of the optimal torque control method in practical controllers. Nevertheless, this control strategy lacks speed error terms and adjustable parameters for convergence speed, posing significant challenges for system analysis and improvement.

This paper analyzes the aerodynamic torque of the wind turbine rotor at various wind speeds and the torque-speed operation trajectories of the generator at each maximum power tracking point. Based on the principle that the aerodynamic torque of the wind turbine rotor balances the generator torque at the maximum power point, a calculation method for the dynamic optimal rotational speed based on the electromagnetic torque of the generator is proposed. Taking this optimal rotational speed as the control target, a speed-torque closed-loop controller is designed, and the control effects in the constant rotational speed region and variable rotational speed region are analyzed. Finally, the control strategy is simulated and field-tested.

## 2 The Maximum Power Point Tracking (MPPT) Principle of Wind Turbines

The aerodynamic power captured by the wind turbine rotor from wind energy is:

$$P = 0.5\rho Sv^3 C_p(\lambda, \beta) \quad (1)$$

where:  $\rho$  is the air density;  $S$  is the wind turbine rotor swept area;  $v$  is the wind speed at the hub center;  $C_p(\lambda, \beta)$  is the wind energy utilization coefficient;  $\beta$  is the pitch angle;  $\lambda$  is the tip - speed ratio.

Based on the  $C_p - \lambda$  characteristic curves of the wind turbine rotor under different pitch angles, when the pitch angle is set to the optimal value  $\beta_{opt}$  (typically 0 degree), as illustrated in Figure 1, there exists a unique optimal tip-speed ratio  $\lambda_{opt}$ , which corresponds to the maximum power coefficient  $C_{pmax}$ .

Therefore, the principle of maximum power point tracking below the rated wind speed is that when the wind speed  $v$  changes, the generator speed  $\omega_g$  is real-time adjusted to make the wind turbine rotor operate at the maximum wind energy utilization coefficient point  $C_{pmax}$ , so as to achieve maximum power point tracking. The captured maximum wind energy is shown in equation (2):

$$P = 0.5\rho Sv^3 C_{pmax}(\lambda_{opt}, \beta_{opt}) \quad (2)$$

By dividing both sides of Equation (2) by the generator rotational  $\omega_g$  and incorporating the definition of the tip-speed ratio, the optimal aerodynamic torque  $T_a$  (referred to the high-speed shaft) can be expressed as:

$$T_a = k_{opt}\omega_{opt}^2 \quad (3)$$

Where:  $k_{opt} = 0.5\rho\pi R^5 C_{Pmax} / (G\lambda_{opt})^3$  is called the optimal modal gain coefficient;  $G$  is the gearbox speed ratio;  $\omega_{opt}$  is the  
 95 optimal generator speed.

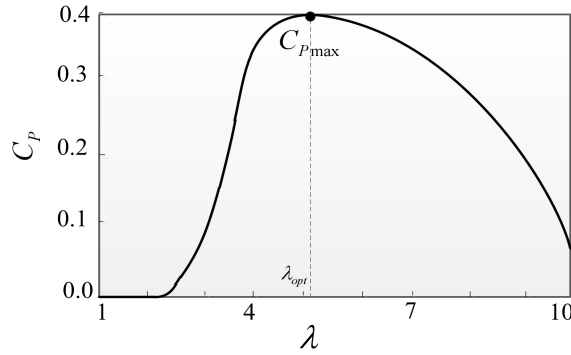


Figure 1.  $C_P$  vs  $\lambda$  curve for wind turbine

## 2. Maximum Power Control Method Based on Direct Speed Control

### 2.1 Optimal Rotational Speed Estimation Method

100 By analyzing Equation (3), the corresponding optimal generator speed  $\omega_{opt}$  can be derived from the steady-state aerodynamic torque  $T_a$ :

$$\omega_{opt} = \sqrt{\frac{T_a}{K_{opt}}} \quad (4)$$

However, for wind turbines in actual operation, aerodynamic torque is difficult to measure. Cardenas-Dobson et al. (1996) and Camblong et al. (2006) propose a maximum power point tracking method based on direct speed control, in which the optimal rotational speed is calculated based on real-time observed aerodynamic torque. Nevertheless, aerodynamic torque  
 105 observation is complex and time-consuming, and slight disturbances can affect the speed setpoint of the controller, making it impractical in engineering. By analyzing the aerodynamic torque curve of the wind turbine rotor and the steady-state speed-torque operation trajectory of maximum power tracking, this paper proposes a calculation method for dynamic optimal rotational speed based on the electromagnetic torque of the generator.

Figure 2 shows the steady-state speed-torque curve of a variable-speed variable-pitch wind turbine during maximum power point tracking, where the horizontal axis represents the generator angular velocity and the vertical axis represents torque. The curve ABQEF indicates the generator torque values during maximum power tracking operation of the wind turbine.  
 110

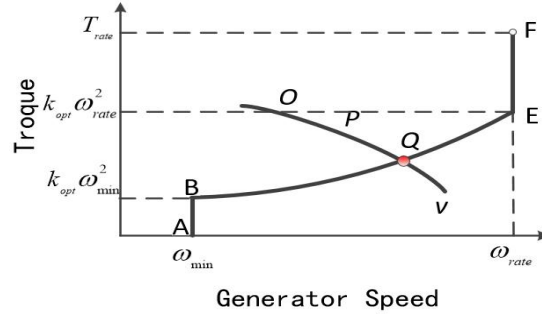


**Figure 2. Torque-speed stable curve for variable speed pitch regulated wind turbine**

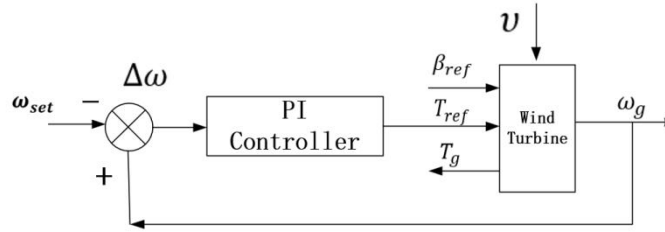
In Figure 2, when the wind speed is  $v$ , the aerodynamic torque of the wind turbine rotor is represented by the curve OPQ  
 115 (Burton et al., 3rd ed.). The intersection point of this rotor aerodynamic torque curve and the generator optimal torque curve  
 BQE is Q. That is, after the wind turbine reaches steady-state operation, the aerodynamic torque  $T_a$  of the rotor is numerically  
 equal to the generator torque  $T_g$ . Therefore, the optimal rotational speed  $\omega_{opt}$  can be approximated as:

$$\omega_{opt} = \sqrt{\frac{T_g}{K_{opt}}} \quad (5)$$

Since the electromagnetic torque of the generator can be easily obtained from the converter communication interface, the  
 unmeasurable aerodynamic torque can be observed by the measurable electromagnetic torque. Therefore, the optimal rotational  
 120 speed can be obtained through Equation (5).

## 2.2 Design of Direct Speed Controller Based on Optimal Speed

After obtaining the real-time optimal generator speed  $\omega_{opt}$ , a closed-loop controller based on the optimal speed can be designed.  
 As shown in Figure 3, the optimal generator speed is used as the set speed  $\omega_{set}$  of the controller. The deviation between  $\omega_{set}$   
 and the current generator speed  $\omega_g$  is input into the speed controller. Here, the speed controller adopts a Proportional-Integral  
 125 (PI) controller, which calculates and outputs a torque reference value  $T_{ref}$  to the wind turbine converter. This is the Direct  
 Speed Control (DSC) method described in this paper. In Figure 3,  $v$  is the wind speed,  $\beta_{fine}$  is the optimal pitch angle, and  $T_g$   
 is the generator electromagnetic torque. Since the response speed of the converter is in the millisecond level,  $T_g$  is generally  
 approximately equal to  $T_{ref}$ .



130 **Figure 3. Block diagram of direct speed control based on optimal speed**

Since wind turbines typically have two constant-speed operating points below the rated wind speed (as shown by line segments AB and EF in Figure 2), the calculated optimal generator speed  $\omega_{opt}$  at the rated wind speed must be limited by the minimum generator speed  $\omega_{min}$  and the rated generator speed  $\omega_{rate}$ , i.e.,

If  $\omega_{opt} \leq \omega_{min}$ , i.e:

$$\omega_{set} = \omega_{min} \quad (6)$$

135 If  $\omega_{opt} \geq \omega_{rate}$ , i.e:

$$\omega_{set} = \omega_{rate} \quad (7)$$

## 2.3 Control Effect Analysis

### 2.3.1 Analysis of Effects in Constant Rotational Speed Region

The constant rotational speed region includes two intervals: the minimum rotational speed region and the rated rotational speed region. Here, the control effect analysis is carried out by taking the minimum rotational speed region as an example.

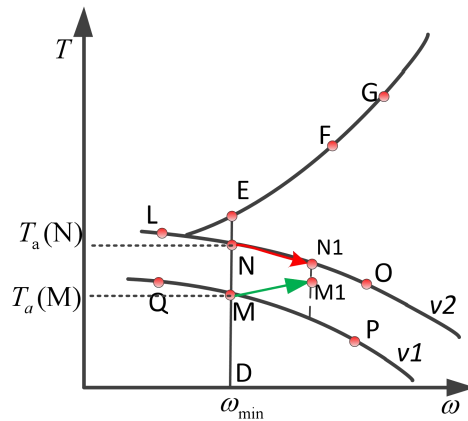
140 Figure 4 is a schematic diagram for the control effect analysis in the minimum rotational speed region, where the horizontal axis represents the generator speed and the vertical axis represents torque. The straight line ED indicates the operating interval of the minimum generator speed. The curve QMP shows the relationship between the rotor aerodynamic torque and speed at wind speed  $v_1$ , while the curve LNO represents this relationship at wind speed  $v_2$  (where  $v_2 > v_1$ ). The curve EFG is the quadratic curve of optimal torque control.

145 When the wind speed is  $v_1$ , the wind turbine operates at the steady-state working point M, where the generator speed is  $\omega_{min}$ , the aerodynamic torque is  $T_a(M)$ , and the generator torque  $T_g(M)$  is equal to  $T_a(M)$ . Suppose at a certain moment, the wind speed suddenly changes from  $v_1$  to  $v_2$ , and the aerodynamic torque also suddenly changes to  $T_a(N)$ . Since the generator torque remains  $T_g(M)$  at this time, and  $T_a(N) > T_g(M)$ , the generator speed increases. At this time, the aerodynamic speed moves from point N to point O on the aerodynamic curve LNO. Assuming that it moves to point O at the next control cycle T, the  
 150 generator speed is  $\omega_o$  at this time. The optimal generator speed calculated by the controller according to equation (6) is less than  $\omega_{min}$  so the speed setpoint  $\omega_{set}$  of the direct speed controller shown in Figure 4 is  $\omega_{min}$ . Since  $\omega_g - \omega_{set} = \omega_o - \omega_{min} > 0$ , the speed PI controller increases the output of the generator torque  $T_g$  setpoint based on this positive deviation. Since the



generator speed setpoint calculated by Equation (6) for the aerodynamic torque  $T_a$  corresponding to wind speed  $v_2$  at different rotational speeds is always  $\omega_{min}$ , according to the rotational speed differential equation  $\frac{d\omega}{dt} = T_a - T_g$ ,  $T_a$  and  $T_g$  need to reach equilibrium. The wind turbine drive train will eventually stabilize at point N, where the generator speed is  $\omega_{min}$ , the aerodynamic torque is  $T_a(N)$ , and the generator torque  $T_g(N)$  equals the aerodynamic torque.

If the wind speed suddenly changes from  $v_2$  to  $v_1$  the analysis can also be carried out by this method. The control effect in the rated rotational speed region is similar to that in the minimum rotational speed region.



160 **Figure 4. Schematic diagram of control effect analysis in minimum speed zone**

### 2.3.2 Variable-Speed Region Performance Analysis

Figure 5 illustrates the control performance in the variable-speed region, with axes and curve definitions consistent with Figure 4. Here, the wind speed  $v_4$  is greater than  $v_3$ .

When the wind speed is  $v_3$ , the wind turbine operates at the steady-state working point M, where the generator speed is  $\omega_1$ , the aerodynamic torque is  $T_a(M)$ , and the generator torque  $T_g(M)$  is equal to the aerodynamic torque  $T_a(M)$ . Suppose at a certain moment, the wind speed suddenly changes from  $v_3$  to  $v_4$ , and the aerodynamic torque also suddenly changes to  $T_a(N)$ . Since the generator torque remains  $T_g(M)$  at this time, and  $T_a(N) > T_g(M)$ , the generator speed increases. At this moment, the aerodynamic speed moves from point N to point O along the aerodynamic curve LNO.

When the wind speed is  $v_4$ , under this DSC control strategy, there are two conditions for the wind turbine to operate stably at the working point:

① The aerodynamic torque  $T_a$  is equal to the generator torque  $T_g$

$$T_a = T_g \tag{8}$$

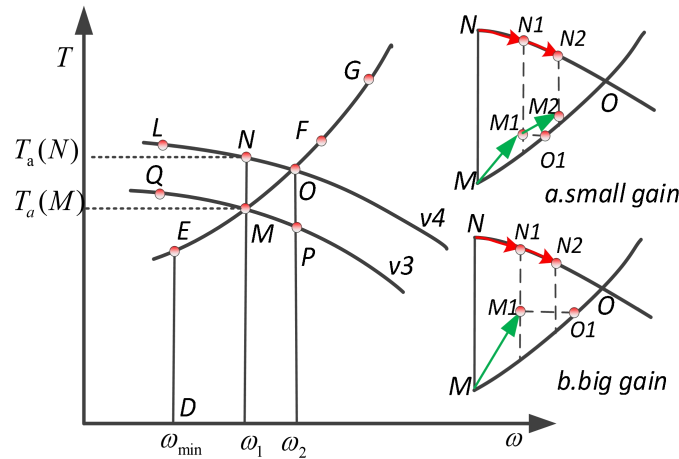
② The speed setpoint  $\omega_{set}$  of the speed controller is:



$$\omega_{set} = \sqrt{\frac{T_g}{K_{opt}}} \quad (9)$$

By rearranging Equation (9), the generator torque  $T_g$  can be derived as:

$$T_g = K_{opt}\omega_{set}^2 \quad (10)$$



175

**Figure 5. Schematic diagram of control effect analysis in variable speed zone**

Since the actual rotational speed is equal to the speed setpoint when the speed controller is in stable operation, it can be seen from Equation (10) that the generator torque and speed operate on the quadratic curve EFG. Therefore, the stable operating point is the intersection point O of the aerodynamic torque curve LNO and the quadratic curve EFG.

Figure 5a further analyzes the process of how the operating point moves from point M to point O. Suppose that at the next control cycle T1, the aerodynamic torque curve of the wind turbine rotor moves from point N to point N1, and the generator speed at this time is denoted as  $\omega_{n1}$ . At this T1 moment, the controller calculates the speed setpoint  $\omega_{set} = \omega_n$  of the controller based on the generator torque  $T_g$  at the previous control cycle T0. Since  $\Delta\omega = \omega_{n1} - \omega_{set} = \omega_{n1} - \omega_n > 0$ , the speed PI controller increases the increment of the generator torque  $T_g$  according to this positive deviation, and the generator torque  $T_g$  given by the controller moves to point M1. According to this motion law, the aerodynamic torque continues to move toward the equilibrium point O, and the generator torque finally also moves to point O, reaching a new steady-state equilibrium point.

### 2.3.3 Analysis of the Influence of Different Control Parameters on the Control Effect in the Variable Speed Region

To analyze the influence of different control parameters of the speed controller on the control effect in the variable speed region, it is assumed that different controller gains are used. Figure 5a represents a smaller gain, and Figure 5b represents a larger gain.



190 In Figure 5a, point O1 is the intersection of the horizontal line passing through point M1 and the quadratic curve EFG , and point N2 is the operating point of the rotor aerodynamic curve at the T2 control cycle. Since the abscissa corresponding to point N2 is larger than that of point O1 , the speed controller's deviation  $\Delta\omega$  at time T2 remains greater than 0. With an appropriate PI controller gain,  $\Delta\omega$  can remain positive before reaching the stable operating point O , ensuring that the generator torque value given by the speed controller increases monotonically without torque or power oscillations.

195 In Figure 5b, point O1 is also the intersection of the horizontal line passing through point M1 and the quadratic curve EFG, and point N2 is the operating point of the rotor aerodynamic curve at the T2 control cycle. Here, the abscissa corresponding to point N2 is smaller than that of point O1 , so the speed controller's deviation  $\Delta\omega$  is less than 0 at time T2 . It can be seen that with a larger PI controller gain,  $\Delta\omega$  will switch between positive and negative values before reaching the stable operating point O. As a result, the generator torque value given by the speed controller will oscillate, and the power will also undergo small-scale fluctuations accordingly.

200 Therefore, in the variable speed range, the speed controller is relatively sensitive to the gain value. Appropriate parameters should be selected when designing the controller.

### 3 Simulation Verification

The wind turbine used for simulation verification is a 1.5 MW variable-speed variable-pitch wind turbine, and its main parameters are shown in Table 1. The direct speed control strategy (DSC) is simulated and studied using MATLAB.

**Tab.1 Technical parameters of wind turbine**

Wind turbine types	Rotor Diameter (m)	Rated Power (kW)	Rated Wind Speed (m/s)
Horizontal-axis upwind turbine	92	1500	9.03
Cut-in Wind Speed (m/s)	Cut-out Wind Speed (m/s)	Gearbox Ratio	Optimal Pitch Angle (°)
3.0	25	70.58	0
Types of Generators	Minimum Grid-Connected Speed / RPM	Rated Speed / RPM	Rated Torque of Generator / Nm
Squirrel-cage Asynchronous Generator	700	1000	14325
Maximum Wind Energy Utilization Coefficient	Optimal Tip Speed / rad	Optimal Modal Gain / (Nm/(rad/s) <sup>2</sup> )	
0.5	10	0.563313	



### 3.1 Simulation of Gradually Varying Wind Conditions in the Minimum Rotational Speed Zone

210 When the wind speed is greater than 3 m/s but less than  $\omega_{min}R/(G \times \lambda_{opt})$  4.7 m/s , the wind turbine operates in the minimum rotational speed zone.

The settings for the simulated gradient wind time series are as follows: starting at 70s, the wind speed linearly increases from 3.5m/s to 4.5m/s over 20s, remains constant for 120s, and then linearly decreases back to 3.5m/s over another 20s. The wind speed variation process is shown in Figure 6a.

215 The aerodynamic torque of the wind turbine will change with the variation of wind speed. During the wind speed increase process, as the aerodynamic torque of the wind turbine increases, the balance with the generator torque is broken, so the generator speed also gradually increases at 70s, as shown in Figure 6b. However, according to the optimal speed estimation method described in Section 2.1, the speed setpoint is still set to the minimum generator speed of 700 RPM. From this moment on, the input deviation  $\Delta\omega$  of the speed controller is a positive value greater than 0, so the generator torque output by the  
220 controller also begins to increase, as shown in Figure 6c.

As the wind speed gradually increases, the aerodynamic torque of the wind turbine remains greater than the generator torque, causing the generator speed to keep increasing. As shown in Figure 6b, the generator speed increases by approximately 8 RPM during this process. The speed disturbance in this phase depends on the gain of the speed controller, and the speed disturbance value can be reduced by increasing the gain. When the generator torque also increases to 1514 Nm as shown in Figure 6c, it  
225 balances with the aerodynamic torque of the wind turbine. At this point, the generator speed is adjusted back to the set target value of 700 RPM through the feedback of the controller.

At the 210s mark, the wind speed starts to decrease, causing the aerodynamic torque of the wind turbine to decrease accordingly. As a result, the generator speed drops. However, the speed setpoint remains at the minimum generator speed. Since the input deviation  $\Delta\omega$  of the speed controller becomes negative, the generator torque output by the controller also begins  
230 to decrease. When the generator torque and aerodynamic torque reach equilibrium again, the generator speed stabilizes at the minimum generator speed of 700 RPM.

Figure 6d shows the generator power, indicating that the generator power changes with the wind speed. Therefore, the DSC control strategy can operate stably in the minimum speed region. Additionally, in this region, when the wind speed decreases, it may cause the generator speed to drop too rapidly (e.g., at the 224s moment in Figure 6d). To prevent the generator from  
235 under - speeding and shutting down due to excessive speed reduction, the controller gain can be appropriately increased.

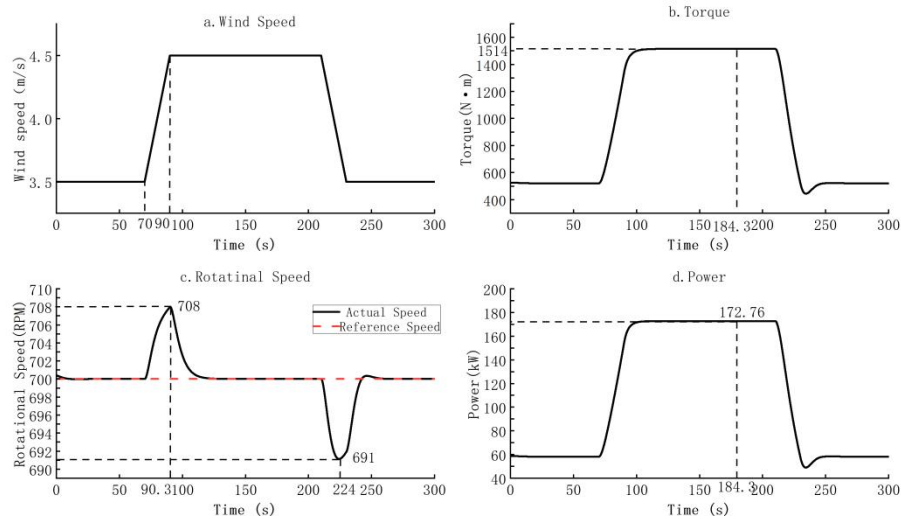


**Fig. 6 Simulation result in gradient wind case in the minimum speed zone**

### 3.2 Simulation of Variable - Speed Region under Gradient Wind Conditions

When the wind speed is greater than approximately  $\omega_{min}R/(G \times \lambda_{opt})$  4.7 m/s but less than approximately  $\omega_{max}R/(G \times \lambda_{opt})$  8.2 m/s, the wind turbine operates in the variable - speed region.

As shown in the simulation results of Figure 8, when the wind speed increases from 5.5 m/s to 8.0 m/s, remains constant for 120 seconds, and then decreases back to 5.5 m/s, the following observations can be made: During the initial 65-second steady-state operation at 5.5 m/s, the generator torque remains around 2700 Nm while both the set value and actual operating speed of the generator maintain 720 RPM. Calculations indicate that the turbine operates at a tip-speed ratio of 9 under these conditions, which deviates from the optimal tip-speed ratio listed in Table 1. The failure to achieve maximum wind energy capture is attributed to the fact that neither the rotational speed nor wind speed has reached their rated values.

Figure 8(e) demonstrates that the maximum wind energy utilization coefficient ( $C_p$ ) represents the ratio of generator power to the energy potential of effective wind speed at the rotor. Notably, during the 65-second initial steady-state operation at 5.5 m/s, the maximum  $C_p$  value reaches 0.49, slightly lower than the theoretical maximum of 0.5 shown in Table 1. This discrepancy arises because the  $C_p - \lambda$  curve in Figure 1 specifically characterizes aerodynamic power at the rotor, whereas actual wind turbine systems typically substitute this with generator power measurements. The generator power inherently includes mechanical and electrical losses from the drivetrain, resulting in a relatively lower calculated  $C_p$  value.

Starting from the 65-second mark, as the wind speed gradually increases to 8.0 m/s, the aerodynamic torque of the wind turbine also rises, as shown in Figure 8b. During this process, since the aerodynamic torque exceeds the current generator torque, the generator speed begins to increase. Analysis of Figure 8c reveals that throughout the speed acceleration phase, the actual generator speed consistently remains higher than the controller-set generator speed. As a result, the input deviation of the speed controller ( $\Delta\omega$ ) remains greater than zero, prompting the generator torque setpoint to continuously increase. This

adjustment persists until the generator torque matches the aerodynamic torque, at which point the drivetrain reaches a new equilibrium state.

260 During the wind speed reduction phase, the process operates inversely compared to the speed increase phase. The input deviation of the speed controller ( $\Delta\omega$ ) becomes negative ( $\Delta\omega < 0$ ), leading to a continuous decrease in the generator torque setpoint. This adjustment persists until the generator torque matches the aerodynamic torque, at which point the drivetrain stabilizes at a new equilibrium.

In engineering applications, to mitigate such transient dynamics, it is common practice to use wind speed data from relatively  
 265 stable intervals for statistical analysis or to employ averaged data over 30 seconds or 10 minutes for processing. These approaches effectively reduce the impact of rapid fluctuations. Notably, the average wind energy utilization coefficient (CP) over the 300-second interval in this study is calculated as 0.49, indicating that the wind turbine achieves maximum power point tracking (MPPT) in the variable-speed region. However, this average CP value is approximately 5% lower than that reported in Reference (LOU Y L et al., 2018) [19] for indirect torque control methods in the same operating region. The discrepancy  
 270 primarily stems from the higher efficiency of the doubly-fed induction generator (DFIG) used in Reference (LOU Y L et al., 2018) [19], which outperforms the squirrel-cage induction generator (SCIG) adopted in this study by several percentage points.

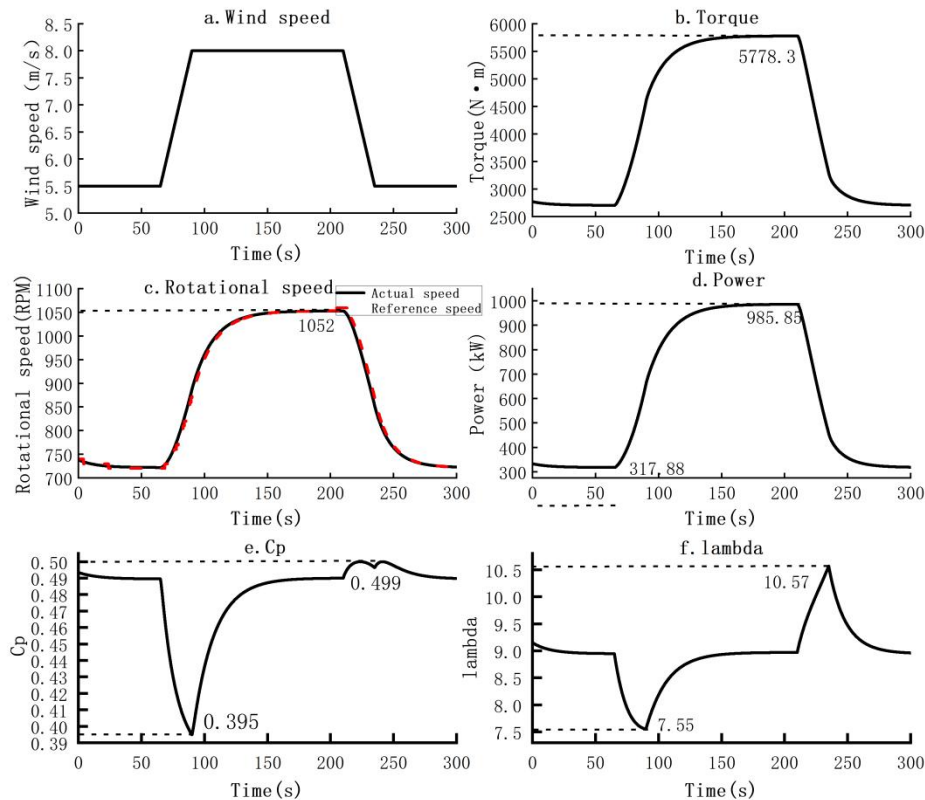


**Fig. 7 Simulation results of gradual wind conditions in variable wind speed zone**



### 3.3 Maximum Speed Region Operation Simulation

275 When the wind speed is greater than approximately  $\omega_{max}R/(G \times \lambda_{opt})$  8.2 m/s but less than 9.3 m/s, the wind turbine operates in the maximum speed region.

When the simulated wind speed increases from 8.4 m/s to 9.2 m/s, remains constant for 140 seconds, and then drops back to 8.4 m/s, the simulation results in Figure 8 show the following: Initial Steady-State Operation (64 s at 8.4 m/s): The generator torque is approximately 6300 Nm, and the generator speed setpoint is 1110 RPM, with the actual speed stabilizing at this value.

280 The calculated tip speed ratio (TSR) during this period is 8.9, which differs from the optimal TSR in Table 1. The failure to achieve maximum wind energy capture is attributed to the fact that neither the rotational speed nor the wind speed has reached their rated values. Maximum Wind Energy Utilization Coefficient  $C_p$ : As defined in Figure 8e,  $C_p$  represents the ratio of generator power to the energy contained in the effective wind speed of the wind turbine. During the initial 64 s steady-state operation at 8.4 m/s, the maximum  $C_p$  is 0.49, lower than the theoretical maximum  $C_p$  of 0.5 in Table 1. This discrepancy

285 occurs because: The  $C_p - \lambda$  curve in Figure 1 corresponds to the aerodynamic power of the wind turbine, which is difficult to directly measure in practical wind turbine systems. Generator power (used as a substitute) incorporates mechanical and electrical losses in the drive train, leading to a lower numerical value.

Starting from the 64th second, as the wind speed gradually increases to 9.2 m/s, the aerodynamic torque of the wind turbine increases accordingly, as shown in Figure 8b. During this process, since the aerodynamic torque exceeds the current generator

290 torque, the generator speed begins to rise. Analyzing Figure 8c reveals that during the speed increase, the actual generator speed always remains higher than the speed set by the controller. Therefore, the input deviation  $\Delta\omega$  of the speed controller is greater than 0, causing the generator torque command value to continuously increase until the generator torque matches the aerodynamic torque and the drive train reaches a new equilibrium point. At the 235th second, the generator torque is 6658.61 Nm, the generator speed is 1149.31 RPM, and the wind energy utilization coefficient is 0.496, indicating that the wind turbine

295 has achieved maximum power point tracking operation.

During the wind speed decrease process, which is the reverse of the speed increase process, the input deviation  $\Delta\omega$  of the speed controller becomes negative. Consequently, the generator torque command value continuously decreases until the generator torque equals the aerodynamic torque, at which point the drive train reaches a new equilibrium state.

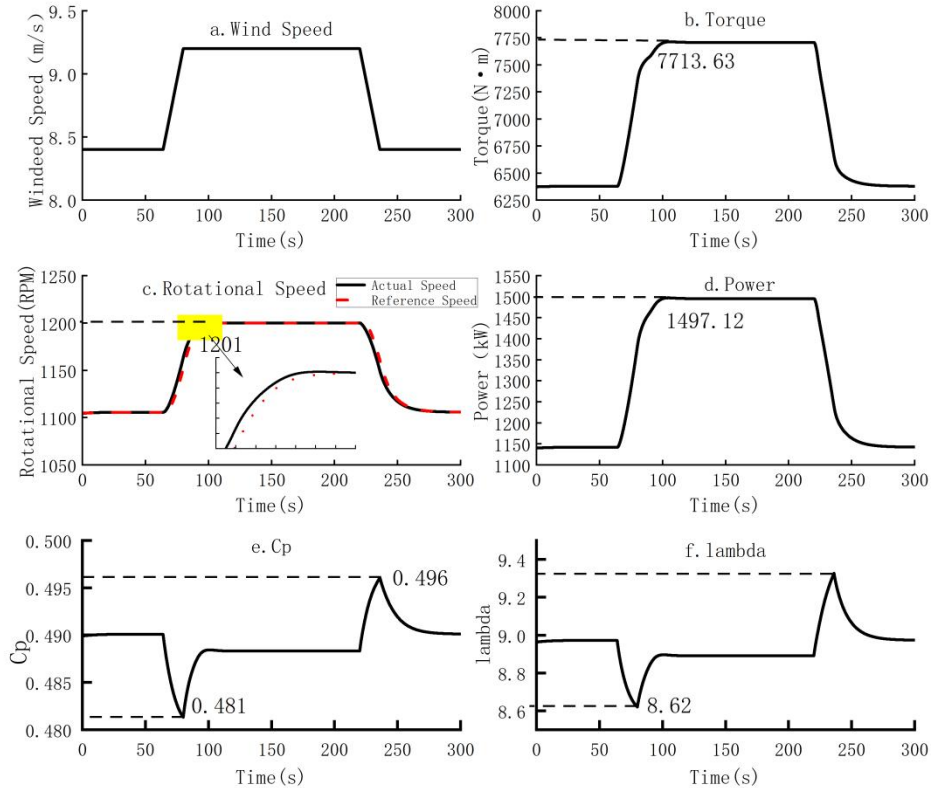


**Fig. 8 Simulation results under maximum speed range operating conditions**

300

### 3.4 Simulation of Variable-Speed Region under Turbulent Wind Conditions

Figure 9a depicts the wind speed with an average value of 10.0 m/s and a turbulence intensity (Ti) of 18.34%, under which the wind turbine operates in the variable-speed region. Analyzing the data from 90 s to 110 s in Figures 9c and 9d, it is observed that both the speed setpoint and torque value of Controller B exhibit small-amplitude oscillations. This phenomenon arises because the relatively high gain of Controller B causes the speed deviation  $\Delta\omega$  to switch between positive and negative values before reaching the stable operating point, leading to oscillations in the generator torque command from the speed controller and consequent fluctuations in power. In contrast, Controller A with a lower gain shows a monotonic change in  $\Delta\omega$  without oscillations before settling at the stable point. This result aligns with the theoretical analysis in Section 2.3.3 of this paper, indicating that in the variable-speed region, the speed controller is sensitive to the gain value, and appropriate parameter selection is crucial during controller design.

305

310

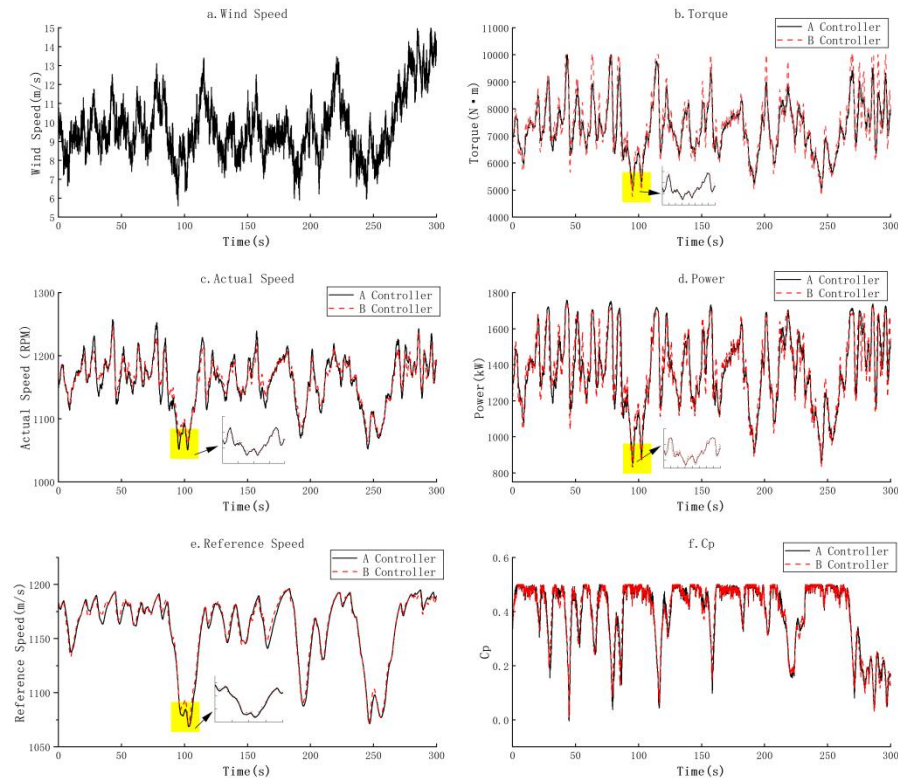
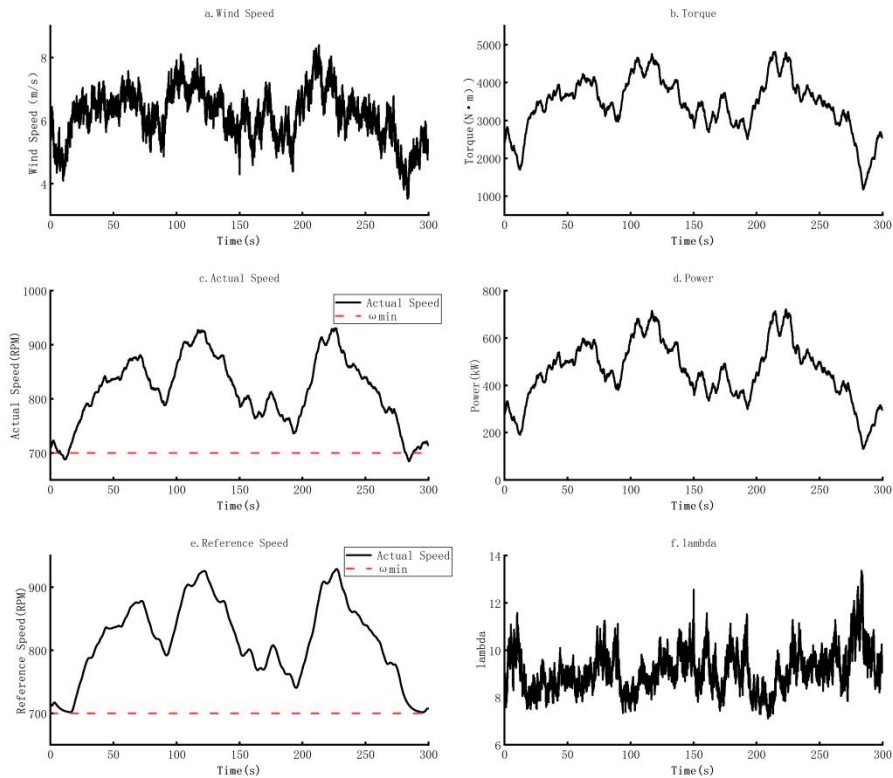


**Fig. 9** Simulation results of turbulent wind conditions in variable wind speed zone

#### 4 Field Validation of Control Strategies

315 After the direct speed control strategy was tested and simulated in a laboratory system, the PLC controller code was written, and wind farm testing and verification were carried out on a certain 1.5MW prototype. The wind turbine equipped with this control strategy has operated stably for 6 months.

320 A segment of the unit's operating data below the rated wind speed was collected, as shown in Figure 10. It can be seen that the main operating parameters, such as the generator operating speed and its setpoint, generator torque, and power, all follow the direct speed control law without any control failure. During the period of 60 s to 120 s, the wind speed is approximately 4 m/s, and the unit operates in the minimum speed range with the speed setpoint at 720 RPM. The actual generator speed fluctuates around 720 RPM. In other periods, the controller operates in the variable-speed region, achieving smooth switching between the constant-speed region and the variable-speed region.



325

**Fig. 10 Field test results in turbulent wind**

Further analysis of the 220 s–250 s time interval, where the average wind speed is 6.49 m/s and the instantaneous wind speed varies between 5 m/s and 7 m/s, shows that the unit operates in the variable-speed region. By dividing the generator power in this interval by the energy contained in the wind speed at the corresponding moment, the wind energy utilization coefficient curve shown in Figure 11 is obtained. The average  $C_p$  in this interval is 0.49, which is close to the average value of 0.49 in the gradient wind simulation of Section 3.2. This indicates that the control strategy maintains the wind energy utilization coefficient at an optimal level to ensure maximum wind energy utilization. The test results verify that the direct speed control strategy can achieve maximum power point tracking.

330

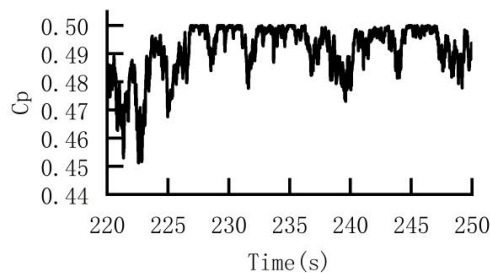




**Fig. 11 Data analysis results of maximum utilization coefficient of wind energy**

## 335 5 Conclusions

Aiming at the problems of the traditional optimal torque control strategy, such as lacking speed tracking error term, having non-adjustable convergence speed, and invalid control logic in the constant speed zone, this paper proposes a direct speed control strategy for MPPT of wind turbines. Through theoretical analysis, simulation verification and field tests, the following conclusions are drawn:

- 340 1) Based on the principle of the balance between aerodynamic torque and generator torque at the maximum power point of wind turbines, a dynamic optimal speed estimation method is proposed, which uses measurable generator electromagnetic torque to replace the difficult-to-directly-observe aerodynamic torque. This method solves the engineering application problem of traditional direct speed control relying on complex aerodynamic torque observation, and achieves accurate calculation of optimal speed.
- 345 2) A speed deviation feedback controller with dynamic optimal speed as the set value is designed. By limiting the speed range between the minimum generator speed and the rated generator speed, unified control of the constant speed zone and the variable speed zone is realized. The controller introduces a speed error term and adjustable PI parameters, solving the problem that traditional indirect speed control is difficult to analyze and optimize.
- 3) The full-condition simulation results based on a 1.5 MW variable-speed variable-pitch wind turbine show that the  
350 proposed control strategy can operate stably under gradient wind and turbulent wind conditions in the minimum speed zone, variable speed zone and maximum speed zone, effectively avoiding torque and power oscillation, with the wind energy utilization coefficient stabilized at around 0.49.
- 4) The results of field tests in wind farms show that the wind turbine equipped with this control strategy can operate stably  
355 for more than 6 months, realize smooth switching between the constant speed zone and the variable speed zone, and has the advantages of simple and practical control logic, indicating a good prospect for engineering promotion.

## References

- [1] LIN Z W, CHEN Z Y, WU Q W. Coordinated mechanical loads and power optimization of wind energy conversion systems with variable-weight model predictive control strategy[J]. *Applied Energy*, 2019, 236: 307-317.
- [2] CHEN C Q, LI X R, TAN Z X. Frequency modulation capability of wind storage considering wind power uncertainty[J].  
360 *High voltage engineering*, 2022, 48(6): 2128-2139.
- [3] CHEN J, CEN L H, CAO A K, et al. An improved optimal torque control of wind turbine considering actual large rotational inertia[J]. *Acta energiae solaris sinica*, 2021, 42(6): 297-303.
- [4] LOU Y L, CAI X, YE H Y, et al. Optimal generation research of wind turbine based on power decoupling near rated wind speed[J]. *Power system technology*, 2019, 43(3): 879-886.



- 365 [5] ZHOU L J, Li Q, YIN M H, et al. Torque Curve Gain Dynamic Optimization for Maximum Power Point Tracking of Wind Turbines[J]. Transaction of China Electro technical Society, 2023, 1-14.
- [6] FATHABADI H. Maximum mechanical power extraction from wind turbines using novel proposed high accuracy single-sensor-based maximum power point tracking technique[J]. Energy, 2016, 113: 1219-1230.
- [7] ABDULLAH M A, YATIM A H M, TAN C W, et al. A review of maximum power point tracking algorithms for wind energy systems[J]. Renewable and sustainable energy reviews, 2012, 16(5): 3220-3227.
- 370 [8] TIAN D, HUANG M Y, TANG S Z, et al. Output power and tower load control of large-scale wind turbines based on active disturbance rejection control[J]. Acta energiae solaris sinica, 2023, 44(5): 466-472.
- [9] YE H Y. Control technology of wind turbine[M]. 3rd ed. Beijing: China Machine Press, 2015.
- [10] FATHABADI H. Novel Maximum Electrical and Mechanical Power Tracking Controllers for Wind Energy Conversion Systems[J]. IEEE Journal of Emerging and Selected Topics in Power Electronics, 2017, 5(4).
- 375 [11] APATA O, OYEDOKUN D T O. An overview of control techniques for wind turbine systems[J]. Scientific African, 2020, 10: e00566.
- [12] WANG Y, YANG W, LAN Y S, et al. Adaptive tuning method for optimal tip speed ratio control parameters of large offshore wind turbines[J]. Ship engineering, 2019, 41(S1): 334-336, 340.
- 380 [13] VOLOSENESCU C. A Comparative Analysis of Some Methods for Wind Turbine Maximum Power Point Tracking[J]. Mathematics, 2021, 9(19).
- [14] ZOUHEYR D, LOTFI B, ABDELMADJID B. Improved hardware implementation of a TSR based MPPT algorithm for a low cost connected wind turbine emulator under unbalanced wind speeds[J]. Energy, 2021, 232: 121039.
- [15] ZHANG Y, HAN J G, TANG T H. Simulation Research on MPPT Controlling of Wind Turbine Based on Hill-climbing Algorithm[J]. Journal of Shanghai Institute of Technology (Natural), 2012, 12(02): 152-156.
- 385 [16] ZHANG X L, LI Q, YIN M H, et al. An improved hill-climbing searching method based on halt mechanism[J]. Proceedings of the CSEE, 2012, 32(14): 128-134.
- [17] ZHANG H. Maximum power point tracking control of wind turbine based on efficiency index optimizing torque gain coefficient[D]. Nanjing: Nanjing University of Science and Technology, 2019.
- 390 [18] YANG X J, LIU G. Analysis of the optimization measures on improving energy output of MITA system[J]. Wind energy, 2014(2): 108-111.
- [19] LOU Y L, CAI X, YE H Y, et al. Optimal generator study based on torque follow-up control for wind turbine[J]. Transactions of China electrotechnical society, 2018, 33(8): 1884-1893.
- [20] CARDENAS-DOBSON R, ASHER G M, ASHER G. Torque Observer for the Control of Variable Speed Wind Turbines Operating Below Rated Wind Speed [J]. Wind Engineering, 1996, (4): 20.
- 395 [21] CAMBLONG H, DE ALEGRIA I M, RODRIGUEZ M, et al. Experimental evaluation of wind turbines maximum power point tracking controllers[J]. Energy conversion and management, 2006, 47(18/19): 2846-2858.
- [22] BURTON T, JENKINS N, SHARPE D, et al. Wind energy handbook[M]. 3rd ed.